Estudios Geológicos, 69(1)
enero-junio 2013, 21-34
ISSN: 0367-0449
doi:10.3989/egeol.40879.176

Origin and nature of the aluminium phosphate-sulfate minerals (APS) associated with uranium mineralization in triassic red-beds (Iberian Range, Spain)

Origen y naturaleza de los minerales fosfato-sulfato alumínicos (APS) asociados a la mineralización de uranio en los red-beds triásicos (Cordillera Ibérica, España)

R. Marfil[1], A. La Iglesia[2], J. Estupiñan[3]

ABSTRACT

This study focuses on the mineralogical and chemical study of an Aluminium–phosphate–sulphate (APS) mineralization that occurs in a clastic sequence from the Triassic (Buntsandstein) of the Iberian Range. The deposit is constituted by sandstones, mudstones, and conglomerates with arenaceous matrix, which were deposited in fluvial to shallow-marine environments. In addition to APS minerals, the following diagenetic minerals are present in the clastic sequence: quartz, K-feldspar, kaolinite group minerals, illite, Fe-oxides-hidroxides, carbonate-sulphate cement-replacements and secondary uraniferous minerals. APS minerals were identified and characterized by optical microscopy, X-ray diffraction, scanning electron microscopy, and electron microprobe. Microcrystalline APS crystals occur replacing uraniferous minerals, associated with kaolinite, mica and filling pores, in distal fluvial-to-tidal arkoses-subarkoses. Given their Ca, Sr, and Ba contents, the APS minerals can be defined as a solid solution of crandallite-goyacite-gorceixite (0.53 Ca, 0.46 Sr and 0.01 Ba). The chemical composition, low LREE concentration and Sr > S suggest that the APS mineral were originated during the supergene alteration of the Buntsandstein sandstones due to the presence of the mineralizing fluids which causes the development of U-bearing sandstones in a distal alteration area precipitating from partially dissolved and altered detrital minerals. Besides, the occurrence of dickite associated with APS minerals indicates they were precipitated at diagenetic temperatures (higher than 80ºC), related to the uplifting occurred during the late Cretaceous post-rift thermal stage.

Keywords: APS minerals, U-bearing sandstones, Diagenesis, Triassic Buntsandstein, Iberian Range, Spain.

RESUMEN

Este estudio se centra en el estudio mineralógico y químico de una mineralización de fosfato de aluminio y sulfato (APS) que se produce en una secuencia clástica del Triásico (Buntsandstein) de la Cordillera Ibérica. El depósito está constituido por areniscas, lutitas y conglomerados con matriz arenosa, que fueron depositados en ambientes de fluvial a marino somero. Además de los minerals APS, los minerales diagenéticos siguientes están presentes en la secuencia clástica: cuarzo, feldespato potásico, minerales del grupo de la caolinita, illita, óxidos-hidróxidos de Fe, cemento sulfatado-carbonatado de sustitución y minerales secundarios uraníferos. Los minerales APS fueron identificados y caracterizados por microscopía óptica, difracción de rayos X, microscopía electrónica de barrido, y microsonda electrónica. Los microcristales APS reemplazan a minerales uraníferos, asociados con caolinita, mica y poros de relleno en arcosas-subarcosas fluviales a mareales distales. Dado su contenido en Ca, Sr, y Ba, los minerales APS se pueden definir como una solución sólida de crandallite-goyacite-gorceixite (0,53 Ca, Sr y Ba 0,46 0,01). La baja concentración en LREE y Sr S> sugieren que los minerales APS se originaron durante la alteración supergénica de las areniscas del Buntsandstein debido a la presencia de los fluidos mineralizantes que provocan el desarrollo de areniscas con U en una zona de alteración distal precipitando a partir de

[1] Dpt. de Petrología y Geoquímica, Facultad de Ciencias Geológicas, UCM, 28040 Madrid, Spain. Email: marfil@geo.ucm.es
[2] Instituto de Geociencias (CSIC, UCM), Facultad de Ciencias Geológicas, UCM, 28040 Madrid, Spain. Email: iglesia@geo.ucm.es
[3] Dpt. de Ciencias de la Tierra, Facultad de Ciencias del Mar y Ambientales UCA, 11510 Cádiz, Spain. Email: jenny.estupiñan@uca.es

minerales alterados detríticos. Además, la aparición de dickita asociada a minerales APS indica que se precipitaron a temperaturas diagenéticas (superior a 80 ° C), en relación con el levantamiento que tuvo lugar durante la etapa térmica post-rift en el Cretácico tardío.

Palabras clave: minerals APS minerals, areniscas uraníferas, Diagénesis, Triasico Buntsandstein, Cadena Ibérica, España.

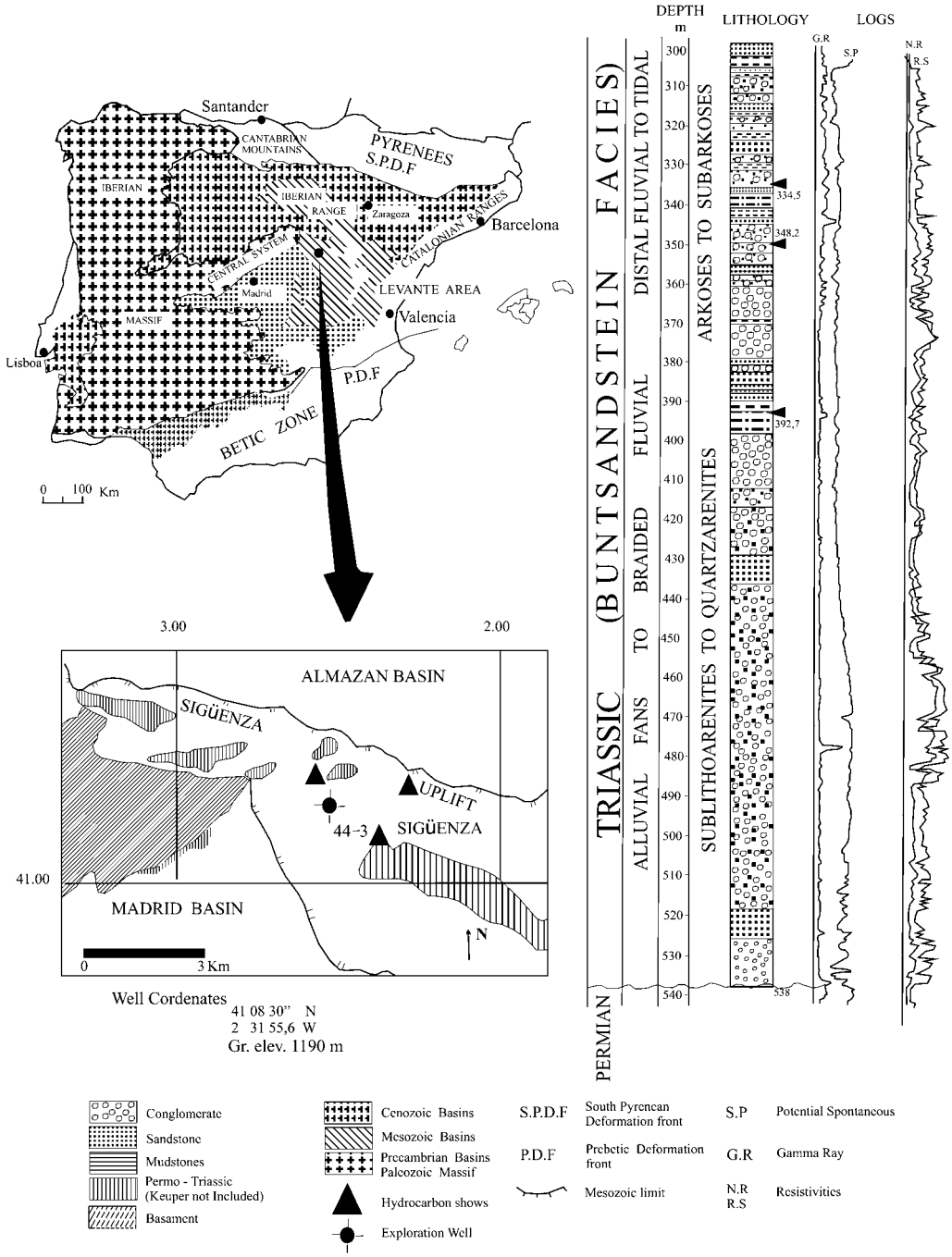

Fig. 1.—Map of Spain showing the location of the Sigüenza High and borehole "Sigüenza 44-3", as well as, the synthetic lithological section of the Triassic (Buntsandstein) sequence with logs (GR, SP, RS). Modified from Marfil *et al.*, (1996b).

Introduction

Aluminium phosphate-sulphate (APS) minerals occur in a wide range of geological environments, ranging from superficial weathering through sedimentary, diagenetic, hydrothermal and metamorphic environments, to post-magmatic systems (Dill, 2001). But, APS minerals have been neglected by geologists and geochemists due to their extremely small sizes (< 0.1-10 μm) and their low concentrations, generally less than 0.05 wt % (Gaboreau *et al.*, 2007). Nevertheless, APS minerals are abundant in the clay mineral host-rock alteration assemblages associated with some uranium areas in the middle Proterozoic basins (Wilson 1985; Beaufort *et al.*, 2005; Gaboreau *et al.*, 2005; Gaboreau *et al.*, 2007) and complex APS minerals were identified by Spötl (1990) as an early diagenetic precipitation in the Late Permian sandstones of the Northern Calcareous Alps (Austria). The model proposed for their origin suggests the precipitation of APS minerals as a consequence of the dissolution of detrital apatite in low pH environment. In an extensive review, Dill (2001) remarked that the precipitation of these minerals indicates extreme acid and oxidising conditions at shallow depths, and describes that these are common occurrences in different geological settings. This origin was also proposed by Benito *et al.*, (2005) and Galán Abellán *et al.*, (2008) who studied the APS minerals group in palaeosols from the southeastern continental Late Permian of the Iberian Range. According to these authors, APS mineral formation occurred shortly after sedimentation, due to the circulation of acid meteoric groundwaters, and concluded that the lack of carbonates and the presence of APS minerals at the base of the Triassic are a clear indication of extremely acid conditions during the Permian-Triassic transition in the studied area.

In Australian sedimentary formations of marine sandstones, Rasmussen (1996) described the presence of authigenic APS minerals (florencite, crandallite, gorceixite) as volumetrically minor but widespread components of Archaean to Cretaceous sandstones. In these sediments trace quantities of crandallite and gorceixite, as well as florencite, occur within pockets and linings of detrital clay and quartz surfaces. According to this author, the authigenic minerals were precipitated shortly after burial within the zone of sulphate reduction and methanogenesis. In the Permo-Triassic sandstones of Australia, the above author described early-diagenetic REE-phosphate minerals with crandallite and gorceixite crystals lining cavities formed in the sandstones after grain dissolution. Phosphates were probably formed by the release of P and REE to the pore waters of fluvio-marine sediments, but they could also be formed by the partial dissolution and alteration of detrital minerals (monazite, clay matrix, feldspars and mica). The above considerations confirm that APS minerals are key minerals, and as Gaboreau *et al.*, (2005) asserted, there is a need of more systematic analysis in all types of environments and particularly in siliciclastic sedimentary basins. Similarly, few data is available on the APS compositional variations in relations to the uranium deposits (e.g. Quirt *et al.*, 1991; Gaboreau *et al.*, (2005). The presence of APS minerals in the Buntsandstein sandstones where the uranium mineralization is widespread (Castañon *et al.*, 1981; De la Cruz *et al.*, 1987), is important because the timing of APS precipitation is clearly related to the composition and circulation of the mineralizing fluids. The study of the clays mineralogy of the Buntsandstein in this area of the Iberian Range by SEM, XRD, DTG and DTA has recently been accounted by Marfil *et al.*, (2012) and reveals the illite-dickite-kaolinite mineral assemblage. The purpose of the present study is to contribute to a better understanding of the origin of these APS minerals and their relationship to the uranium mineral alteration.

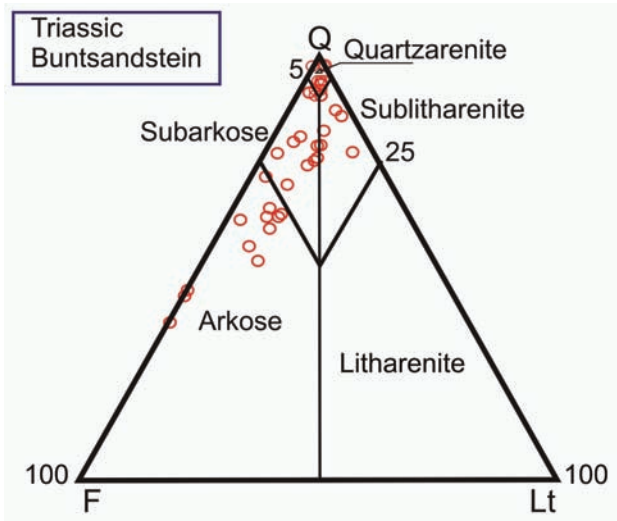

Fig. 2.—Ternary plot of the framework minerals: quartz (Q), feldspars (F) and lithic rock fragments (Lt) for Buntsandstein sandstone samples from borehole Sigüenza SS-44-3.

Table 1.—**Mineral compositions based on modal analyses of selected samples containing APS minerals. Q: cuarzo; K-F: K-feldspar; MRF: metamorphic rock fragments; VRF: Volcanic rock fragments; Q overg: Quartz overgrowth: Anh: anhydrite;**

Sample	Depth (m)	Q %	K-F %	Musc. + Biot. %	MRF %	VRF %	Q overg. %	Calcite + Dolomite %	Clay matrix %	Fe-oxides %	Others
SS-4	316.75	31	21	4	4	-	2	36	1	1	4% Anh; 2% K-F cement
SS-16	351.40	70	12	5	3	-	3	2	3	2	1% K-F cement; <1% Barite
SS-20	365.20	63	17	3	9	-	3	-	3	2	2% Crandallite;
SS- 21	378.40	78	5	3	5	-	2	-	4	3	10% Crandallite,
SS- 24	390.15	75	6	2	2	-	3	-	11	1	2% Crandallite; <1% Chert
SS- 36	467.40	68	3	4	7	2	3	-	10	3	<1% crandallite
SS- 41	502.00	80	2	2	3	1	2	1	7	2	
SS-52	567.40	26	9	1	2	-	-	56	3	3	2% Anhydrite; 6% Plag.

Geological setting

The Iberian Range is an intracratonic, folded segment of the Alpine chain that developed as a rift basin between Permian and late Cretaceous times (Salas & Casas, 1993; Salas *et al.*, 2001). The former authors indicate that the Iberian Basin was filled with thick clastic sequences during two rifting cycles, the first spanning from Late Permian to Late Triassic, and the second from Late Jurassic to Early Albian. During these active periods, sedimentation took place mainly in alluvial to lacustrine environments in a complex system of extensional basins. Both cycles gave way to periods of post-rift thermal subsidence during which shallow-marine carbonates were deposited. The sedimentation of the Permian and Triassic red-bed sandstones and mudstones took place during the first stage of rifting in half–graben basins. During Early Permian (Autunian) times, a series of half–graben, intermontane basins become unfilled by alluvial fans, slope breccias and lacustrine deposits associated in their lower part with volcaniclastic rocks of cal-alkaline affinities, such as andesites with subordinate rhyolites and basalts (Muñoz *et al.*, 1983).

The Buntsandstein sediments can be divided into two major successions that are not always both present in the Iberian area: a lower one, comprising laterally restricted conglomerates and more widespread sandstones, and an upper one of irregular distribution, comprising sandstones, sandstones and siltstones and siltstones. The lower succession shows a marked fining –upward sequence interpreted as being of alluvial fan origin and forming an apron derived from an elevated SW margin of the riff basin. The overlying formation consists, of pink to red bedded sandstones of sandy braided river origin. These sandstones consist of amalgamate channel deposits totally devoid of fine grained flood plain sediments and are interpreted as having been deposited during a slow subsidence rate (Lopez-Gomez et al, 2011).

This study is based on core samples from borehole “Sigüenza 44-3” (drilled by the former Spanish Junta de Energía Nuclear (today CIEMAT) and by the Shell Company in 1978), with a depth of 999 m. This borehole is located on the Sigüenza High some 110 km Northeast of Madrid (Fig. 1). Two large Buntsandstein units were sampled, a lower unit (538 to 369 m) composed of conglomerates

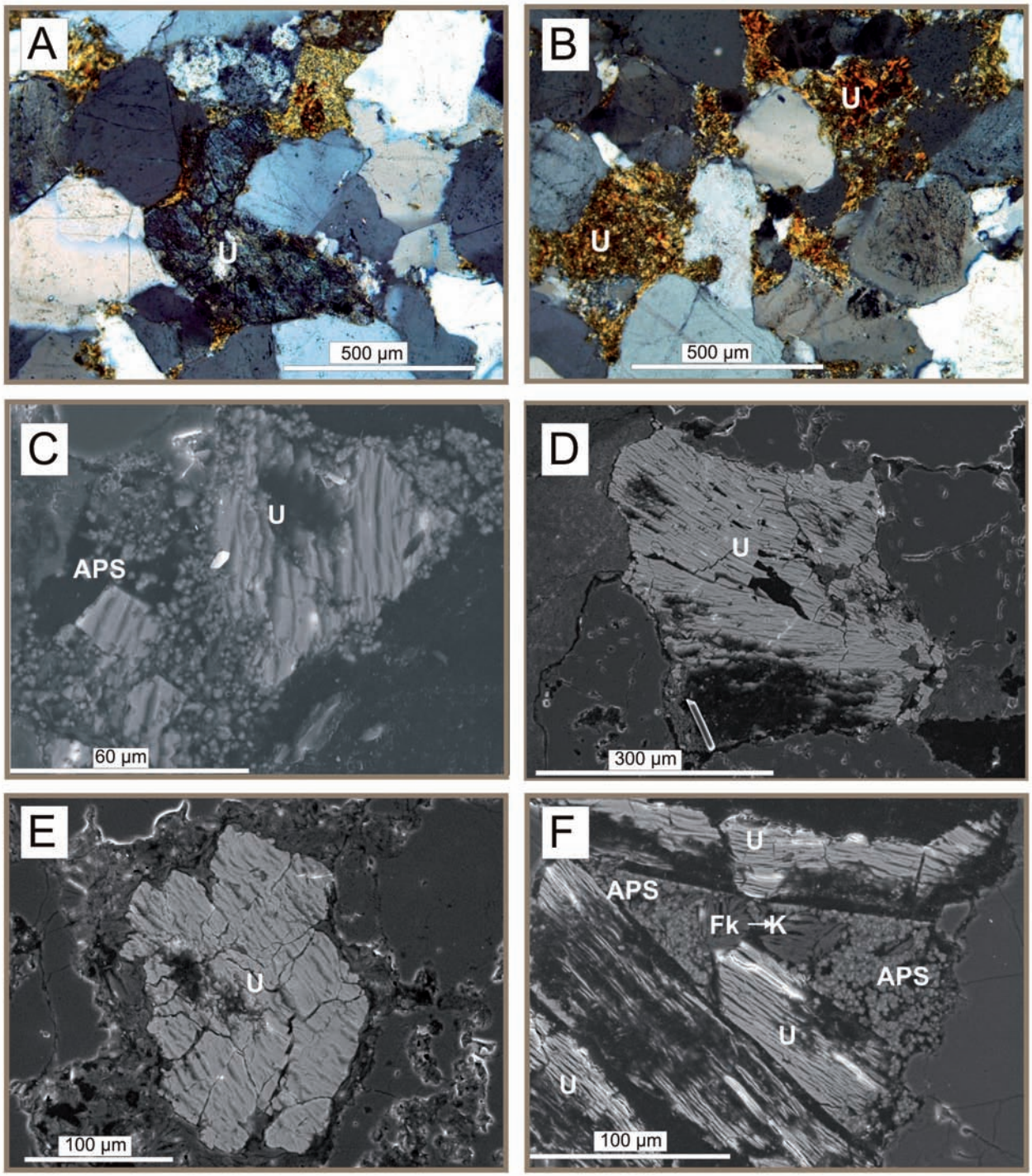

Fig. 3.—A) Photomicrograph (crossed nicols) of a subarkosic sandstone showing frequent quartz overgrowths and K-feldspars replaced by kaolin minerals. (Small rests of feldspar are yellow stained). B) SEM image of abundant matrix of fibrous illite and a more recent phase of coarse dickite crystals (D). Some of these crystals are intergrowth with quartz cement, (Qc). C) Photomicrograph (crossed nicols) showing secondary uranium minerals (U) replacing frame-work detrital grains (possibly feldspars and clay matrix), as well as, quartz overgrowths (Qc). D) SEM image of the secondary uranium mineral (U) partially replaced by APS (Table 4, analysis 67617-5). E) and F) SEM images of secondary uranium mineral grains (U). F) U grain is replacing clay matrix composed by kaolinite. The analyses of these grains are in Table 4 (analysis 20492-1 and 67616-3)..

Table 2.—**Mineralogical composition by XRD diffraction of selected sandstone samples (size fraction 2-20 μm).**

Sample	Depth (m)	Quartz %	K- Feldspar %	Mica (I+I/S) %	Kaolinite %	Dolomite %	Calcite %	Hematite %	Others
SS-16	351.4	22	17	43	14	2	1	1	Barite, Dolomite
SS-20	365.2	14	5	62	10	-	-	4	5% Crandallite
SS-21	378.4	13	7	29	25	-	-	1	25% Crandallite
SS- 24	390.15	13	10	48	27	-	-	2	1% Crandallite
SS- 36	467.4	20	0	54	23	-	-	3	
SS- 41	502.0	10	1	63	26	-	-	-	
SS- 54	572.6	13	4	47	32	-	-	4	Dolomite

and sandstones with sporadic interbedded mudstones at the top, and an upper unit (369 to 300 m) constituted by sandstones and mudstones and occasional conglomerates with arenaceous matrix. Both units are red beds, separated by a 10 m-thick conglomerate, and were sedimentologically distinguished in the original survey logs (Fig. 1). The Gamma ray spectrometry shows a radioactive anomaly at a depth between 340 and 345 m, which is related to the presence of secondary uranium minerals in grey mineralized zones. On the contrary, in this area, exploration of Buntsandstein targets has not been successful, despite the fact that surface oil seeps are present in the Sigüenza area (Marfil *et al.*, 1996b).

Samples and methods

The mineralogical composition of the almost 50 sandstones and mudstones selected from the two Buntsandstein units was determined by modal analysis (400 points per thin section) using a polarizing microscope. X-ray powder diffraction (XRD) analyses were performed on the 2-20 μm and <2μm fractions. A Bruker D8 Advance diffractometer, equipped with a Sol-X detector was used. The experimental conditions were: measurement interval 2- 70º 2θ, time per step1 s, and a step size of 0.02º 2θ. The mineneralogical composition of the crystalline phases was estimated following Chung´s (1975) method and using Bruker software (EVA). Selected by XRD 5 sandstones and mudstones samples were examined using a JEOL JSM-6400 scanning electron microscope equipped with a Link Systems energy-dispersive X-ray microanalyser (accelerating voltage 15 KV, beam current 3nA) by secondary electron (SE) and backscattered electron (BSE) modes. Finally, the chemical composition of the APS minerals was determined using a JEOL JXA-8900 electron microprobe (accelerating voltage 15 kV, current 21.5 nA, beam diameter 5 μm and the counting time 100s). The detection limits in ppm were 250 for Al, 370 for Sr; 245 for Fe, 205 for P, 135 for Ca, 240 for S, and 285 for Ba. For LREE the detection limits were 222 for Nd, 90 for La, 60 for Ce, 53 for Th and 158 for Pr. The following standard were used: For P apatite; for Ca augite; for Sr CO_3Sr; for Al sillimanite; for Fe almandine; for Ba CO_3Ba, for F apatite; for S chalcopyrite, and for LREE synthetic glass from PH developments.

Results

Bulk composition of the sandstones

Modal analyses indicated that the Buntsandstein sandstones are mainly arkoses, subarkoses and subordinated quartzarenites and sublitharenites (Table 1; Fig. 2) with coarse to medium grain (2.0 - 1.0 mm and 1-0.5 mm), and moderate sorting (Trask coefficient 1.2-1.4). Feldspars, mainly K-feldspars, appear to be commonly replaced by illite

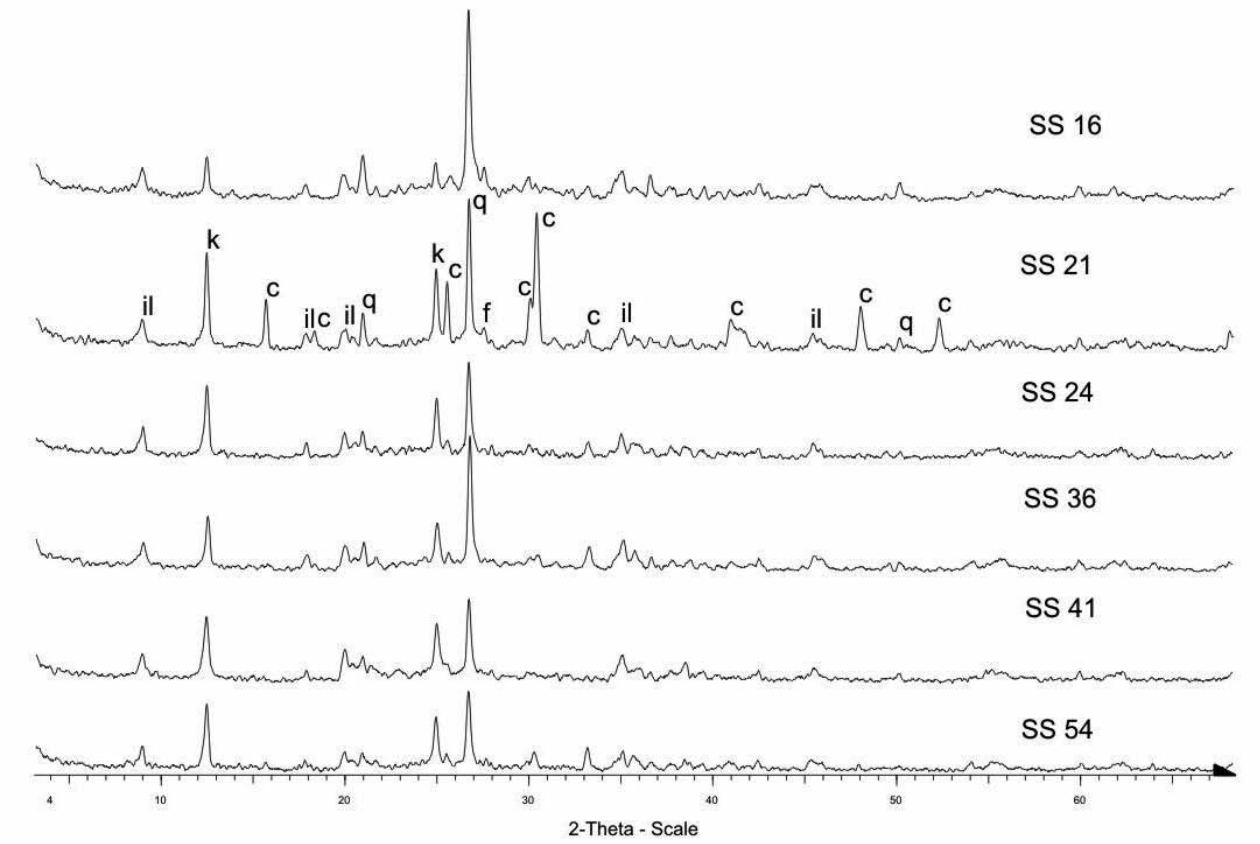

Fig. 4.—A) SEM image of several secondary uranium mineral phases (U) replaced by APS microcrystals. In the centre, remains of K-feldspar partially replaced by kaolinite (F-K to K) (Analyses 67616-4 of Table 4). B) Abundant APS crystals filling fractured quartz grains and replacing kaolinite matrix. C) SEM image of aggregates of small APS euhedral crystals lining the planes of distorted muscovite and corroding quartz, replacing feldspars, and partially filling the pore space. D) SEM image under BSE mode of APS zoned microcrystals filling the porosity and corroding the quartz grains. E) SEM images of sandstone showing kaolinite matrix and very rich in APS crystals. Illite is rarely observed in this area where mica is altered to kaolinite-dickite. F) SEM image showing APS crystals between twisted kaolinite booklets and extremely broken quartz grains.

and kaolinite minerals. Quartz cement occurs as syntaxial overgrowths frequently corroded by clays mainly kaolinite-dickite and fibrous illite (Fig. 3A, B). Ductile rock fragments consist of micaschists, argillites, and early eroded and transported (rip-up) clay clasts. Mica includes muscovite and subordinate amounts of biotite. Turmaline, apatite, rutile, anatase, sphene, malachite, ilmenite, monazite, torbernite and xenotime are characteristic accessory components. Framework grains and the matrix are replaced by secondary uraniferous minerals in green and grey sandstones beds. These secondary uraniferous minerals appear in different associations: as cement and replacing feldspars, illite epimatrix and quartz cement (Fig. 3C), filling microfractures of the quartz grains and the exfoliation planes of the mica. They also become visible as individual grains (Fig. 3D, E, F). Several of these uraniferous mineral grains are replaced by APS as the figures 3D, F and 4A show. Pyrite appears to be associated with the development of anhydrite nodules.. Other cements include scarce K-feldspar overgrowths, Fe and Ti oxides or oxyhydroxides (as coatings and patches), dolomite and Fe-dolomite/ankerite. Occasionally, abundant calcite, anhydrite and barite are common cement replacements. APS minerals are recognized at a depth between 365 m and 390m in core samples, corresponding to distal fluvial-to-tidal arkoses, near the boundary between the upper and lower units of the studied sequence (Fig.1). Hydrocarbon (HC) impregnations were detected in some grey Buntsandstein sandstones (Fig. 1); however, organic matter is rare and only appears in some anhydrite nodules.

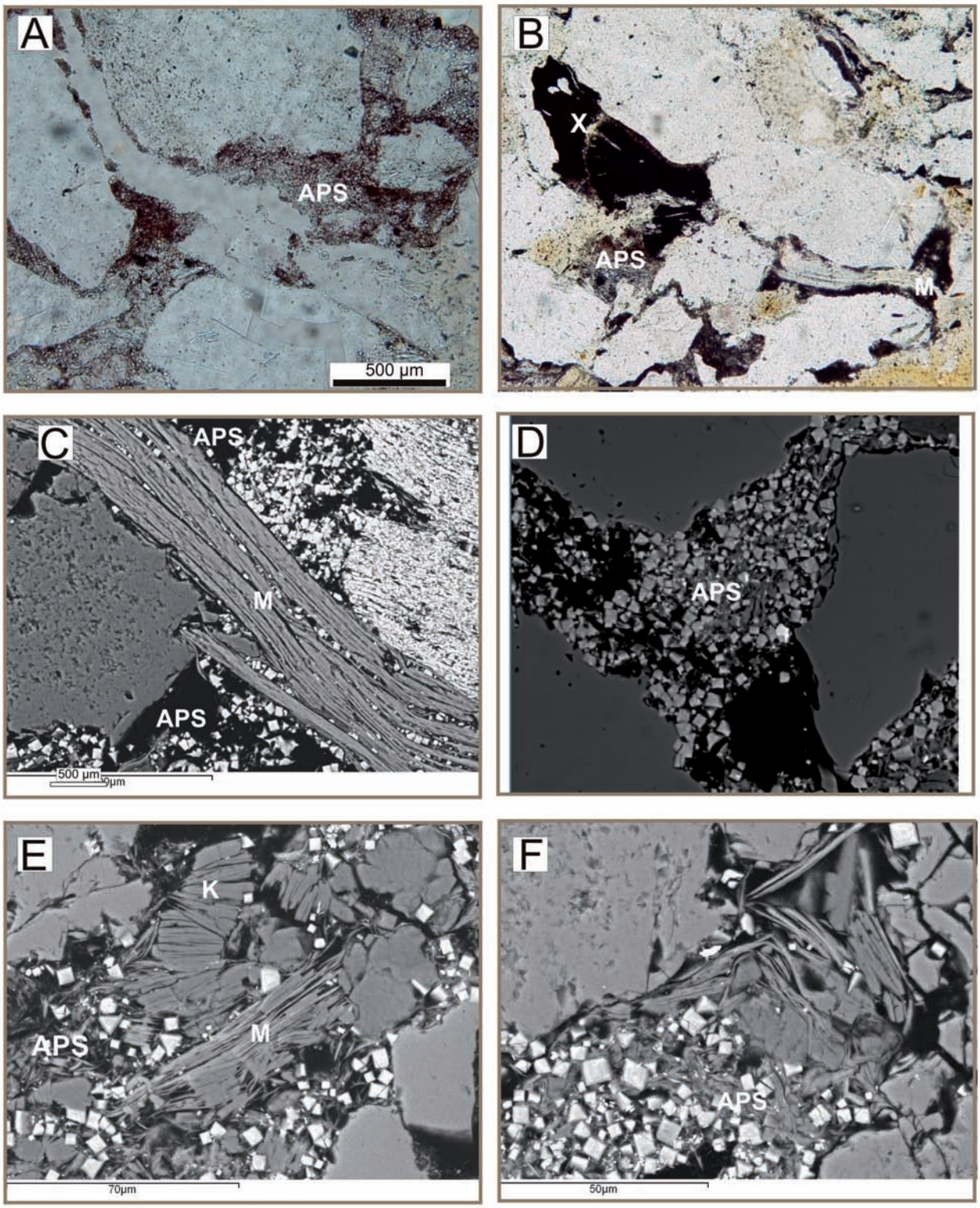

Fig. 5.—Comparison of the XRD patterns of the selected Buntsandstein sandstone samples containing APS minerals from the upper unit (300 to 369 m) and the samples from the lower unit (369 to 538 m). Fraction 20-2µm. The peaks are labeled as c: crandallite, f: feldspar, il: illite, k: kaolinite, q: quartz

Table 3.—**Electron microprobe analyses and structural formulae of APS minerals from the Buntsandstein sandstones**

Sample	1	2	3	4	5	6	7	8	9	10	11	12	13	14	15	16	17	18	19	20	21	22	average
CaO	5,92	6,33	7,03	6,17	5,66	5,88	6,5	5,66	5,77	6,41	6,23	6	6,15	5,05	5,22	5,77	5,88	6,06	5,52	5,31	5,04	5,91	5,88
SrO	10,04	10,09	8,46	11	10,86	9,5	8,92	10,42	10,49	9,93	9,82	9,31	9,17	9,41	9,97	9	9,14	8,93	9,77	9,08	10,88	9,16	9,7
BaO	0,35	0,46	0,47	0,5	0,41	0,43	0,38	0,34	0,48	0,46	0,3	0,36	0,46	0,45	0,32	0,27	0,35	0,31	0,26	0,42	0,34	0,21	0,38
Al_2O_3	33,04	33,59	34,14	34.04	33,67	33,98	34,43	32,82	34,41	33,4	33,83	32,15	33,43	31,86	32,38	34,06	33,61	32,62	33,04	32,38	32,9	31,19	33,19
Fe_2O_3	0,71	0,91	0,67	1,2	0,87	1,32	1,11	1,23	0,88	1,04	0,86	3,03	1,49	0,67	0,5	1,95	1,25	1,38	0,91	0,85	0,74	0,9	1,11
P_2O_5	24,73	24,68	24,34	25,3	25,12	23,91	24,96	24,11	24,06	24,53	24,58	23,39	23,84	22,67	23,87	24,91	24,93	24,43	25,09	23,58	24,28	22,61	24,27
SO_3	6,57	6,61	7,63	8	7,26	7,84	6,12	7,41	8,34	6,7	7,59	6,91	7,13	7,67	7,28	6,95	6,85	5,29	7,44	6,71	7,27	6,4	7,09
F	0,39	0,29	0,25	0,21	0,3	0,26	0,25	0,28	0,33	0,23	0,27	0,32	0,46	0,41	0,44	0,44	0,33	0,35	0,39	0,4	0,46	0,29	0,33
Total	81,75	82,96	82,99	52,38	84,15	83,12	82,67	82,27	84,76	82,7	83,48	81,47	82,13	78,18	79,97	83,35	82,33	79,35	82,41	78,71	81,91	76,67	80,44
Ca	0,48	0,51	0,55	0,48	0,45	0,46	0,5	0,46	0,45	0,51	0,49	0,48	0,49	0,43	0,44	0,45	0,47	0,49	0,45	0,44	0,41	0,51	0,47
Sr	0,44	0,44	0,36	0,47	0,47	0,4	0,37	0,46	0,44	0,43	0,42	0,4	0,39	0,43	0,45	0,38	0,39	0,39	0,43	0,41	0,48	0,43	0,42
Ba	0,01	0,01	0,01	0,01	0,01	0,01	0,01	0,01	0,01	0,01	0,01	0,01	0,01	0,01	0,01	0,01	0,01	0,01	0,01	0,01	0,01	0,01	0,01
Al	2,96	2,95	2,96	2,93	2,95	2,93	2,94	2,93	2,95	2,94	2,95	2,83	2,92	2,96	2,97	2,89	2,93	2,92	2,95	2,95	2,96	2,95	2,94
Fe	0,04	0,05	0,04	0,07	0,05	0,07	0,06	0,07	0,05	0,06	0,05	0,17	0,08	0,04	0,03	0,11	0,07	0,08	0,05	0,05	0,04	0,05	0,06
PO_4	1,59	1,56	1,52	1,57	1,58	1,48	1,53	1,55	1,48	1,55	1,54	1,48	1,49	1,51	1,57	1,52	1,56	1,57	1,61	1,54	1,57	1,53	1,54
SO_4	0,37	0,37	0,42	0,44	0,41	0,43	0,33	0,42	0,46	0,38	0,42	0,39	0,4	0,45	0,43	0,38	0,38	0,3	0,42	0,39	0,42	0,38	0,4
F	0,08	0,06	0,06	0,06	0,06	0,06	0,06	0,07	0,08	0,05	0,06	0,08	0,11	0,1	0,11	0,19	0,08	0,08	0,09	0,1	0,11	0,07	0,08
H	0,74	0,56	0,6	0,71	0,75	0,61	0,54	0,69	0,62	0,55	0,68	0,5	0,59	0,81	0,89	0,85	0,78	0,61	0,99	0,8	0,84	0,57	0,67
OH	6	6	6	6	6	6	6	6	6	6	6	6	6	6	6	6	6	6	6	6	6	6	6

Petrography, mineralogy, and chemical characteristic of the APS minerals

Significant amounts of APS minerals were detected in thin sections and SEM. APS minerals occur as very small idiomorphic crystals filling secondary pores, stylolites and microfractures (Fig. 4 B). These minerals replace uraniferous grains or they are enclosed in the distorted and broken mica crystals (Fig. 4 C). APS crystals (sizes ranging from 5 to 10 μm) also appear filling cavities as cement that surrounds corroded quartz grains (Fig. 4 D). APS minerals are preferentially found among expanded muscovite flakes which are totally twisted by mechanical compaction and altered to kaolinite (Fig. 4E, F). The quartz present in these sandstones has suturated and stylolitic contacts marked by iron oxides, indicative of pressure-solution processes.

The XRD patterns of the 2-20μm fraction of the richest samples in APS minerals (Fig. 5) show a composition of: crandallite 25%, quartz 13%, K-feldspar 7%, mica-illite 29%, kaolin minerals 25% and hematite 1% (Table 2). Crandallite with values less than 10%, was also detected by XRD analyses in the <2 μm size-fraction.

The chemical compositions of the APS minerals and the structural formulae calculated on the basis of 2 moles of (XO_4) and 6 moles of (OH) per formula unit, following Scott´s method (1987), are given in Table 3. According to the criteria of this author, the analysed minerals belong to the plumbogummite group since trivalent anions are >1.5 moles, divalent cations in A-sites are dominant and Al>Fe in B-sites. The results of the analyses are plotted on Scott's diagram (Fig. 6). The calculated average value of $(XO4)^{3-}$ is 1.51, which fits within the plumbogummite field. Considering the contents of Ca, Sr, and Ba, these APS minerals can be defined as a solid solution of crandallite-goyacite-gorceixite (Ca 0.53, Sr 0.46, Ba 0.01). The LREE (La, Ce, Pr, Nd and Th) contents are very low; in the case of La and Ce the average value is 282 ppm and 434 ppm, respectively. The content of Pr, Nd and Th in all the analyzed APS minerals was usually below the detection limit. Table 4 shows the chemical composition of the selected sand grains containing high values in UO_3. Their values in Cu, As and P suggest an uranyl phosphate arseniate, of the autunite group, specifically torbernite-zeunerite serie: $Cu(UO_2)2(PO_4, AsO_4)_2.10H_2O$.

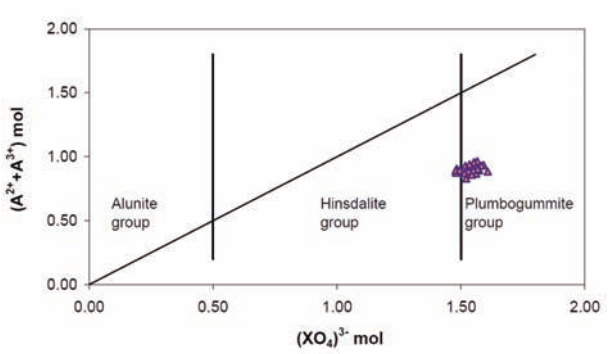

Fig. 5.—Scott´s diagram: trivalent anions in XO 4 sites vs. divalent ± trivalent cations in A sites for APS minerals.

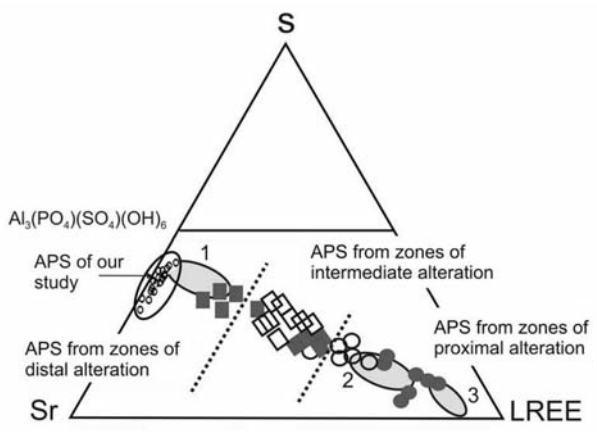

Fig. 6.—Reciprocal diagram based on Sr, S, and LREE electron microprobe analyses for APS minerals from the studied Buntsandstein uraniferous sandstones compared to the APS compositions from the Kombolgie Formation (Gaboreau et al., 2005). Distal alteration zone (1); intermediate alteration zone (2); and zone of proximal alteration (3).

Discussion

The geochemical conditions in the Triassic basin during the APS mineral precipitation were oxidising and slightly acid, as indicated by the presence of the paragenesis formed by kaolinite-illite-quartz and hematite. Furthermore, the red sandstones beds are bleached and mottled corresponding to hematite dissolution caused by repeated process of acidification as described by Hoeve & Quirt (1984) and Kister *et al.*, (2006). According to Rasmussen (1996), the critical factor controlling the APS mineral precipitation is the availability of Al. In the Buntsandstein sandstones, enough Al for the precipitation of APS minerals was supplied by the alteration of feldspars, mica or kaolinite. The Sr

Table 4.—**Representative microanalyses by scanning electron microscopy of the uraniferous grains in three APS bearing samples corresponding to SS-21, SS-23 and SS-24.**

Sample	20492-1	20492-2	20492-3	67616-1	67616-2	67616-3	67616-4	67617-1	67617-2	67617-3	67617-4	67617-5	67617-6
	%	%	%	%	%	%	%	%	%	%	%	%	%
CuO	8,15	6,57	6,22	6,86	5,44	6,75	5,01	7,43	8,21	6,35	5,45	6,48	3,69
UO_3	72,29	74,11	73,29	69,72	73,97	75,78	74,73	73,27	76,09	76,73	77,17	75,32	78,22
ZrO_2	1,81	0,00	0,00	0,00	0,00	0,00	0,00	0,00	0,00	0,00	0,00	0,00	0,00
ThO_2	0,00	0,00	2,88	3,38	2,07	2,16	2,42	0,00	0,00	0,00	0,06	0,00	0,00
Cs_2O	0,00	0,22	0,14	0,00	0,00	0,00	0,00	2,65	0,00	0,00	0,00	0,00	2,41
As_2O_3	17,74	18,31	16,40	18,81	17,32	15,31	15,42	1,08	1,41	0,00	0,85	4,36	11,97
P_2O_3	0,00	0,79	1,08	1,22	1,20	0,00	2,42	15,58	14,29	16,92	16,47	13,85	3,71
Total	100,00	100,00	100,00	100,00	100,00	100,00	100,00	100,00	100,00	100,00	100,00	100,00	100,00

content of the APS minerals could be related to the presence of celestite and strontianite in the interbedded mudstones and sandstones (Morad *et al.* 1992). Consequently, the compaction of the interbedded mudstones could have released the Sr and S needed for the APS mineral precipitation in the most porous sandstones. Another S source may be the sulphates present in fluids expelled from overlying evaporitic formations (Keuper facies). Such conditions are more likely to be associated with the introduction of oxidising meteoric waters during an uplift event in intra-formational unconformities in the Iberian Basin.

Idiomorphic APS crystals grow between the collapsed mica, which is partially altered to kaolinite fans and dickite (Marfil *et al.*, 2012). This implies that APS minerals postdate the mechanical and chemical compaction, indicating that APS were formed during diagenesis. Constraints placed by vitrinite reflectance deduced temperatures from the associated organic matter in the underlying Permian shales of 135 to 159ºC around 900 m depth (Marfil *et al.*, 1996 a, b). In addition, K/Ar age determinations of the associated fibrous illite, indicate that the episode of illitization in the Buntsandstein occurred around 199.6 ± 4.3 M.a. during Lower and Middle Jurassic (Marfil *et al.*, 1996 a). These ages coincide with the period of the most intensive extensional tectonics in this basin coeval with volcanic events (Salas & Casas, 1993). Thus, the above mentioned facts support the hypothesis of a diagenetic origin and high temperature for the APS minerals, similar origin as for these minerals in the Athabasca basin in Canada (Gaboreau *et al.*, 2007). The assemblage of the APS minerals and dickite implies as well high diagenetic temperature rates. According to Ehrenberg *et al.*, (1993) and Mcaulay *et al.* (1994) the transformation kaolinite-dickite occurs at temperatures between 80 and 130ºC. Thus, the mineralizing fluids, related to tectonic events that occurred during the late Cretaceous post-rift thermal stage, were meteoric waters that transported the uranium into the buried red Buntsandstein sandstones. The fluids were enriched in uranium by circulating through granitic and gnessic rocks of the Spanish Central System (Castañon *et al.*, 1981; De la Cruz *et al.*, 1987), or even through Permian volcanic rhyolitic rocks. In this area of the Iberian Range significant Permian deposits composed by rhyolitic rocks (Peña *et al.*, 1977.

Muñoz *et al.*, 1985) crop out. However, the time of the uranium mineralization and the origin and timing of migrating fluids in the Buntsandstein are not yet fully understood.

The low content in LREE of the APS crystals is not indicative of a clear relationship with the uranium mineralization detected in the studied arkosic sandstones. However, the Gamma ray spectrometry (Fig. 1) shows a radioactive anomaly located at a depth of around 340 m, due to the presence of uranium minerals (Marfil *et al.*, 1996b) Nevertheless, in agreement with the origin proposed by Gaboreau *et al.* (2005), APS minerals in the Triassic Buntsandstein facies could be related to the U-bearing arkosic sandstones in a distal alteration area, as shown in figure 7. Plotting the chemical analyses of the studied APS on the Gaboreau *et al.*(2005) diagram, they fit in the area of distal alteration or barren areas. The above authors explain that the chemical variation in APS minerals is influenced by the host-rock lithology. For an equivalent alteration zone, the APS minerals formed in basement rocks are systematically enriched in P and LREE compared with those formed in the sandstones of the barren areas. Monazite (Ce) in the gneissic weathering profiles of the Leucogia area (Papoulis *et al.*, 2004), is partially altered to a Th-silicate with very low concentration of LREE. Likewise, the above authors found that monazite in hydrothermaly altered rhyolitic rocks of Kos Island, were altered to P-bearing crandallite–goyazite and during this alteration process LREE are depleted. The alteration processes that occurred in the studied U-bearing sandstones could be similar to those described by the above mentioned authors.

Conclusions

In the studied Triassic sequence, several levels of the Buntsandstein sandstones contain important concentrations of APS minerals deposited in secondary pores formed by dissolution of the framework grains, mainly feldspars and uraniferous minerals. They appear as well replacing kaolinite-illite matrix, inside microfractures of the quartz grains and between the exfoliation planes of the mica.

APS minerals were precipitated under diagenetic conditions related to the uplifting occurred during the late Cretaceous post-rift thermal stage at high diagenetic temperatures, suggested by the presence of dickite in the studied samples

APS minerals occurred in barren sandstones in zones of distal alteration with low LREE contents, and related to some tectonic event responsible for the introduction of meteoric and mineralizing waters into the buried sediments.

The intergranular clay matrix composed of kaolinite, illite and the feldspars constituted the main Al source, whereas secondary uranium minerals and apatite were the most probable P sources. Fluids migrating from the Permian evaporitic formations, or, more probably, from the overlying Keuper evaporitic facies can account for the Ca, S and Sr contents.

Based on their chemical composition, the APS minerals have been defined as a solid solution of crandallite-goyacite-gorceixite.

ACKNOWLEDGMENTS

This work was supported by projects CCG07-UCM/AMB-2299 and GR35/10-A. Grupo 910404. We wish to acknowledge and thank Shell Spain Company and the former Junta de Energía Nuclear of Spain for giving us access to their samples and data and the authorization to publish this work. We are also indebted to Da Berta de la Cruz from the CIEMAT for their helpful comments of some aspects of the paper and to check the English version. We thank Alfredo Fernández Larios for performing the electron microprobe analyses of the APS minerals, and Eugenio Baldonedo Rodríguez for his valuable help with the SEM analyses. We are grateful to D. X Arroyo for assistance with SEM studies of the uraniferous minerals. Critical reviews from Dr. H.G. Dill and comments by two other reviewers are gratefully acknowledged have helped to improve the manuscript.

References

Benito, M.I.; De La Horra, R.; Barrenechea, J.F.; Lopez-Gomez, J.; Rodas, M.; Alonso-Azcarate, J.; Arche, A. & Luque, J. (2005). Late Permian in the SE Iberian Ranges, eastern Spain: Petrological and mineralogical characteristics and palaeoenvironmental significance. *Palaeogeography, Palaeoclimatology, Palaeoecology*, 229: 24-39. doi:10.1016/j.palaeo.2004.12.030

Beaufort, D., Patrier, P., Laverret, E., Bruneton, P. & Mondy, J. (2005): Clay alteration associated with Proterozoic unconformity-type uranium deposits in the East Alligator River uranium field (Northern Territory, Australia). *Economic Geology*, 100 (3): 515-536. doi:10.2113/gsecongeo.100.3.515

Castañon, A.; De la Cruz, B. & Marfil, R. (1981). Diagenesis de las areniscas uraníferas del Trias de Mazarete (Guadalajara). *Estudios Geológicos*, 37: 149-158.

Chung, F.H. (1975). Quantitative interpretation of X-ray diffraction patterns of mixtures. III. Simultaneous determination of a set of reference intensities. *Journal of Applied Crystallography*, 8: 17-19. doi:10.1107/S0021889875009454

De La Cruz, B.; Marfil, R.; De la Peña, J.A. & Arribas, J. (1987). Procedencia y evolución díagenética de las areniscas Permo-Triásicas de la Cordillera Ibérica (Sierra de Albarracín-Boniches-Talayuelas, provincias de Teruel y Cuenca). *Cuadernos de Geología Ibérica*, 11: 493-514.

Dill, H.G. (2001). The geology of aluminium phosphates and sulphates of the alunite group minerals: A review. *Earth-Science Reviews*, 53: 35-93. doi:10.1016/S0012-8252(00)00035-0

Ehrenberg, S.N., Aagaard, P., Willson, M.J., Fraser, A.R. and Duthie, D.M.L. (1993). Depth-dependent transformation of kaolinite to dickite in sandstones of the Norwegian continental shelf: *Clay Minerals*, 28: 325-352. doi:10.1180/claymin.1993.028.3.01

Gaboreau, S.; Beaufort, D.; Viellard, Ph.; Patrier, P. & Bruneton, P. (2005). Aluminium phosphate-sulphate minerals associated with Proterozoic unconformity-type uranium deposits in the East Alligator River Uranium Field, Northern Territories, Australia. *The Canadian Mineralogist*, 43: 813–827. doi:10.2113/gscanmin.43.2.813

Gaboreau, S.; Cuney, M.; Quirt, D.; Beaufort, D.; Patrier, P.; & Mathieu, R. (2007). Significance of aluminium phosphate-sulfate minerals associated with U unconformity-type deposits: The Athabasca basin, Canada. *American Mineralogist*, 92: 267-280. doi:10.2138/am.2007.2277

Galán-Abellán, A.B.; Fernández, B.J.; López, J.G.; Lago, M.S. J.; & Benito M.M. I. (2008). Early Triassic-Anisian Continental Sediments from SE Iberian Ranges: Sedimentological and Mineralogical Features, *Sociedad Española de Mineralogía*, 9: 105-107.

Hoeve, J. & Quirt, D.H. (1984). Mineralization and host –rock alteration in relation to clay mineral diagenesis and evolution on the middle-Proterozoic Athabasca Basin, northern Saskatchwan, Canada. *Saskatchewan Research Council Technical Report*, 187: p 187.

Kister, P.; Laverret, E.; Quirt, D.; Cuney, M.; Patrier, P.; Beaufort, D. & Bruneton, P. (2006). Mineralogy and geochemistry of the host-rock alterations associated with the shea creek unconformity-type uranium deposits (Athabasca Basin, Saskatchewan, Canada). Part 2. Regional-scale spatial distribution of the Athabasca group sandstone matrix minerals. *Clays and Clay Minerals*, 54, 3, 295-313. doi:10.1346/CCMN.2006.0540302

López-Gomez, J., Arche, A. & Pérez-Lopez, A. (2002). Permian and Triassic in *The Geology of Spain*. W. Gibbons & Moreno, T. Edited by The Geological Society London. 185-212.

Marfil, R., Bonhomme, M.G., De la Peña, J.A., Penha Dos Santos, R., & Sell, I. (1996a) La edad de las ilitas en areniscas pérmicas y triásicas de la Cordillera Ibérica mediante el método K/Ar: Implicaciones en la historia diagenética y evolución de la cuenca. *Cuadernos de Geología Ibérica*, 20: 61-83.

Marfil, R.; Scherer, M. & Turrero, M.J. (1996b). Diagenetic processes influencing porosity in sandstones from the Triassic Buntsandstein of the Iberian Range, Spain. *Sedimentary Geology*, 105: 203-219. doi:10.1016/0037-0738(95)00138-7

Mcaulay,G.E.,Burley, S.D., Fallik, A.E., & Kusznir, N.J. (1994), Paleohydrodynamic fluid flow regimes during diagenesis of the Brent group in the Hutton-NW Hutton reservoirs, contraints from oxygen isotope studies of authigenic kaolinite and reserve flexural modelling: *Clay Minerals*, 29: 609-629. doi:10.1180/claymin.1994.029.4.16

Morad, S.; Marfil, R.; Al-Aasm, I.S. & Gomez-Gras, D. (1992). The role of mixing-zone dolomitisation in sandstone cementation: Evidence for the Triassic Buntsandstein, the Iberian Range, Spain. *Sedimentary Geology*, 80: 53-65. doi:10.1016/0037-0738(92)90031-L

Muñoz, M.; Ancochea, E. Sagredo, J.; De la Peña, J.A.; Hernan, F.; Brandle, J.L. &

Marfil, R. (1985): Vulcanismo Permo-Carbonífero de la Cordillera Ibérica. *X Cong. Inter. de Stratigraphie et de Géologie du Carbonifere*, *Madrid*, 3: 27-52.

Papoulis, D. Tsolis-Katagas, P. & Katagas, C. (2004). Monazite alteration mechanisms and depletion measurements in kaolins. *Applied Clay Science*, 24: 271-285. doi:10.1016/j.clay.2003.08.011

Peña de la, J.A. and Marfil, R. (1975) Estudio petrológico del Pérmico de la Cordillera Ibérica. Zona de Torre La Hija (NE de Molina de Aragón). *Estudios Geológicos*, 31: 513-530.

Putter, T.D., Andre, L., Bernard, A., Dupuis, C., Jedwab, J., Nicaise, D. & Perruchot, A., (2002): Trace elements (Th, U, Pb, REE) behaviour in a criptokarstic halloysite and kaolinite deposit from Southern Belgium: importance of "accessory"mineral formation for radioactive pollutant trapping . *Applied Geochemistry*, 17: 1313-1328. doi:10.1016/S0883-2927(02)00022-7

Quirt, D., Kotzer, T. & Kyser, T.K. (1991): Tourmaline, phosphate minerals, zircon and pitchblende in the Athabasca group: Maw Zone and McArthur River Areas, *Saskatchewan. Saskatchewan Geological Survey Technical Report*, 91 (4): 181-191.

Rasmussen, B. (1996). Early-diagenetic REE-phosphate minerals (florencite, gorceixite, crandallite and xenotime) in marine sandstones: a major sink for oceanic phosphorus. *American Journal of Science*, 296: 601-632. doi:10.2475/ajs.296.6.601

Salas, R. & Casas, A. (1993). Mesozoic extensional tectonics, stratigraphy and crustal evolution during the Alpine cycle of the eastern Iberian Basin. *Tectonophysics*, 228: 33-35. doi:10.1016/0040-1951(93)90213-4

Salas, R.; Guimerá, J.; Mas, R.; Martin-Closas, C.; Melendez, A.; & Alonso, A. (2001). Evolution of the Mesozoic Central Iberian Rift System and its Cenozoic Inversion (Iberian Chain). In P.A. Ziegler, W., avazza,

A.F.H. Robertson and S. Crasquin- Soleau (Eds.), Peri-Thetys Memoir 6. *Mémoires du Muséum national de Histoire Naturelle*, 186: 145-185.

Scott, K.M. (1987). Solid solution in, and classification of, gossan-derived members of the alunite-jarosite family, Northwest Queensland, Australia. *American Mineralogist*, 72: 178-187.

Spötl, C.H. (1990). Authigenic aluminium phosphate-sulphates in sandstones of the Mitterberg Formation, Northern Calcareous Alps, Austria. *Sedimentology*, 37: 837-845. doi:10.1111/j.1365-3091.1990.tb01828.x

Wilson, J.A. (1985) Crandallite group minerals in the Helikian Athabasca group in Alberta, Canada. *Canadian Journal of Earth Sciences*, 22: 637-641.

Recibido el 2 de diciembre de 2011
Aceptado el 22 de febrero de 2012
Publicado online el 19 de febrero de 2013